Available online at www.sciencedirect.com
SCIENCE DIRECT®
Geochimica et Cosmochimica Acta 70 (2006) 2530–2539
Geochimica
www.elsevier.com/locate/gca

Inhibition of calcite precipitation by orthophosphate: Speciation and thermodynamic considerations

Yi-Pin Lin *, Philip C. Singer

Department of Environmental Sciences and Engineering, University of North Carolina, Chapel Hill, NC 27599-7431, USA

Received 11 July 2005; accepted in revised form 1 March 2006

Abstract

The inhibition of heterogeneous calcite precipitation by orthophosphate was investigated under four different solution compositions using a pH-stat system. The system composition was designed to maintain a constant degree of supersaturation with respect to calcite, but with different carbonate/calcium ratios and pH values during precipitation. Inhibition in the presence of orthophosphate was found to be more effective at lower carbonate/calcium ratios and lower pH values. With the assumption that the calcite precipitation rate is proportional to the surface concentration of active crystal-growth sites, the reduction in the rate of calcite precipitation by phosphate can be explained by a Langmuir adsorption model using a conditional equilibrium constant and total phosphate concentration. Through a detailed analysis of chemical speciation in the solution phase and calcite surface speciation using chemical equilibrium computer modeling, the "conditional" equilibrium constants obtained at different solution compositions were found to converge to a single "non-conditional" value if only $CaHPO_{4(aq)}^{0}$ was considered in the adsorption reaction. This suggests that $CaHPO_{4(aq)}^{0}$ is the responsible species for inhibition of calcite precipitation because it adsorbs to the surface and blocks the active crystal-growth sites. The standard enthalpy change (ΔH^0) and standard entropy change ($T\Delta S^0$) of the adsorption reaction, determined by experiments performed from 15 to 45 °C, were 58.5 and 98.3 kJ/mol, respectively. The high positive values of the standard enthalpy change and the standard entropy change suggest that the adsorption reaction is an endothermic reaction, chemisorptive in nature, and driven by the entropy change, most likely resulting from the dehydration process that accompanies the adsorption of $CaHPO_{4(aq)}^{0}$ onto the calcite surface.

1. Introduction

Phosphorus exists in natural waters in particulate and dissolved form. It is known that phosphorus is a limiting nutrient for the growth of algae and macrophytes in some fresh water systems and enrichment with phosphorus is associated with toxic algal blooms (Kotak et al., 1995) and lake eutrophication (Schindler, 1974).

Geochemical cycling of phosphorus in natural waters exhibits seasonal variations and the release and uptake of phosphorus by sediments is known to be an important process controlling internal phosphorus cycling in the water column (Jensen et al., 1995; House and Denison, 2002; Evans and Johnes, 2004; Evans et al., 2004). Among all the possible interactions between phosphorus and sediments, adsorption and release of phosphate by iron oxide at the oxic/anoxic boundary in the sediment, and adsorption and co-precipitation of phosphate with calcite are most important processes controlling phosphorus concentration in natural aquatic systems (Jensen et al., 1995; House, 2003). In some waters that are highly supersaturated with respect to calcite, the interaction between calcite and phosphate is considered to be a principal process for removing phosphate, particularly during periods of intense photosynthesis (Dittrich and Koschel, 2002; House, 2003). Successful immobilization of phosphorus has also been artificially achieved by the introduction of calcite seed or lime in eutrophic lakes (Dittrich et al., 1997; Prepas et al., 2001; Berg et al., 2004; Walpersdorf et al., 2004).

* Corresponding author. Present address: Department of Civil and Environmental Engineering, University of Iowa, Iowa City, IA 52242-1527, USA.
E-mail address: yipinlin@engineering.uiowa.edu (Y.-P. Lin).

0016-7037/$ - see front matter © 2006 Elsevier Inc. All rights reserved.
doi:10.1016/j.gca.2006.03.002

Phosphate has long been recognized as an inhibitor of calcite precipitation (Reddy, 1977; Ishikawa and Ichikuni, 1981; Mucci, 1986; Giannimaras and Koutsoukos, 1987; House, 1987; Burton and Walter, 1990). The adsorption of phosphate on the calcite surface blocks active crystal-growth sites and retards calcite precipitation. Several laboratory studies have shown that the adsorption of phosphate onto calcite (De Kanel and Morse, 1978; Giannimaras and Koutsoukos, 1987; van der Weijden et al., 1997; Millero et al., 2001) and the inhibition of calcite precipitation by phosphate (Mucci, 1986; Burton and Walter, 1990) are pH-dependent, suggesting that certain phosphate species are the predominant species interacting with the calcite surface. In an attempt to determine the phosphate species responsible for this phenomenon, however, some studies have focused only on the protonated and deprotonated phosphate species (H_3PO_4, $H_2PO_4^-$, HPO_4^{2-}, and $CaHPO_4^{3-}$) without considering complexation of phosphate with metal ions in solution, such as Ca^{2+}, which was present at high concentrations in these precipitation studies in order to make the solutions supersaturated with respect to calcite (Mucci, 1986; Burton and Walter, 1990). The effect of ionic strength on adsorption is a controversial subject: Giannimaras and Koutsoukos (1987) showed that adsorption decreased with increasing ionic strength, while Millero et al. (2001) reported that adsorption was essentially the same in seawaters with salinities varying from 0 to 35 ppt as long as the concentration of bicarbonate was kept constant. However, both studies, as well as others (House et al., 1986), have shown significant desorption of pre-equilibrated phosphate from calcite in phosphate-free solutions or low phosphate seawater, suggesting that electrostatic interactions may be important in the adsorption of phosphate on the calcite surface.

In a previous study (Lin et al., 2005), we showed that the complexation of anionic natural organic matter with Ca^{2+} facilitates its adsorption on the calcite surface and strongly inhibits calcite precipitation. The objectives of the present study are to: (1) investigate the effects of orthophosphate on the kinetics of heterogeneous calcite precipitation using an initial rate approach; (2) determine the phosphate species responsible for inhibiting calcite precipitation, specifically whether Ca^{2+}-phosphate complexation can be used to explain the interactions between phosphate and calcite with respect to heterogeneous precipitation kinetics; and (3) investigate thermodynamic properties of the responsible reaction(s) by performing experiments at different temperatures.

2. Materials and methods

2.1. Experimental procedures

The calcite precipitation experiments in the presence of different phosphate concentrations were conducted using a pH-stat system in solutions seeded with calcite. The system maintains the target supersaturation state with respect to calcite in the working solution by holding the pH at a constant level through the concurrent injection of equivalent amounts of equimolar $CaCl_2$ and Na_2CO_3 solutions (0.053 M, $I = 0.1$) as calcite precipitates during the course of the experiment (90 min). Reagent-grade calcite (300 mg/L, Fisher Chemical Co.) was introduced to the working solution (500 mL) to initiate heterogeneous calcite precipitation. The specific surface area of the calcite seed was 0.278 m^2/g, as determined by the 3-point N_2-BET method (Brunauer et al., 1938). The pH-stat system was verified to perform satisfactorily in preliminary precipitation experiments using phosphate-free solutions, in which the final Ca^{2+} concentration (determined by 0.01 M EDTA titration with murexide as the indicator) and alkalinity (determined by 0.02 N sulfuric acid titration with bromcresol green-methyl red solution as the indicator) agreed within ±10% of the initial Ca^{2+} concentration and alkalinity. The rates of heterogeneous calcite precipitation were determined for solutions with four different C_T/Ca^{2+} ratios (C_T represents the total inorganic carbon concentration) and temperatures in the absence or presence of orthophosphate (Table 1). All solutions were prepared using reagent-grade chemicals with the same degree of supersaturation ($\Omega = 5.3$), which is defined as:

$$\Omega = \frac{(Ca^{2+})(CO_3^{2-})}{K_{sp}}, \quad (1)$$

where (Ca^{2+}) and (CO_3^{2-}) are the activities of calcium and carbonate ions in the solution, respectively, and K_{sp} is the

Table 1
Solution compositions examined in this study ($\Omega = 5.3$, $I = 0.1$)

Temp (°C)	25	25	25	25	15	35	45
C_T/Ca^{2+}[a]	0.5	1	5	10	1	1	1
$(CO_3^-)/(Ca^{2+})$	0.0022	0.0086	0.23116	0.9997	0.0086	0.0086	0.0086
$NaHCO_3$ (M)	0.004	0.004	0.004	0.004	0.00475	0.00345	0.003
$CaCl_2$ (M)	0.008	0.004	0.0008	0.0004	0.00475	0.00345	0.003
KCl (M)	0.0721	0.0840	0.0935	0.0945	0.081	0.0862	0.088
pH	7.68	7.95	8.67	9.01	7.95	7.95	7.95
Total P (μM)	0, 1, 2, 3	0, 1, 2, 3, 4	0, 1, 3, 5	0, 1, 3, 5	0, 1, 3, 5	0, 1, 3, 5	0, 1, 3, 5

[a] C_T represents the total inorganic carbon concentration.

thermodynamic solubility product of calcite ($K_{sp} = 10^{-8.48}$ at 25 °C). The pH value of the working solution was adjusted to the target level for the desired degree of supersaturation with 0.1 N NaOH or HCl, and ionic strength was adjusted to 0.1 with KCl. All solutions were able to exist in a meta-stable state for at least 4 h without homogeneous nucleation as indicated by the constant pH observed during this period. Phosphate was added to working solutions from a stock solution of Na_2HPO_4 followed by the addition of calcite seed. The change in pH was observed only after the calcite seed was introduced indicating that heterogeneous nucleation on reactor walls and at the water/headspace interface was absent. Details of the pH-stat system and the preparation of the working solutions can be found in Lin and Singer (2005) and Lin et al. (2005).

Typical data generated from the pH-stat system in the presence of phosphate are shown in Fig. 1. Time zero represents the time at which the calcite seed was added to initiate heterogeneous precipitation. A quadratic regression was used to fit the stepwise titrant addition data due to a slight increase in precipitation rate resulted from the increased seed surface area as experiment proceeded. Because dissolved phosphate has been reported to continuously adsorb to the calcite surface or to co-precipitate during the overgrowth of calcite (Mucci, 1986; Burton and Walter, 1990), the initial rate of calcite precipitation was estimated from the initial slope of the titrant addition versus time curve. This approach was used to investigate the effects of the initial dissolved phosphate concentration on the rate of calcite precipitation. The rate of calcite precipitation in such systems has been shown to be proportional to the surface area of the calcite seed (Lin and Singer, 2005); therefore kinetic data reported in this study were normalized by the initial surface area of the seed. The seed materials were collected and dried at 35 °C in an oven for 24 h after the completion of several precipitation experiments. X-ray diffraction (XRD) analysis (Rigaku MultiFlex, Rigaku/MSC) was performed on the dried material to determine the crystalline form of the precipitate.

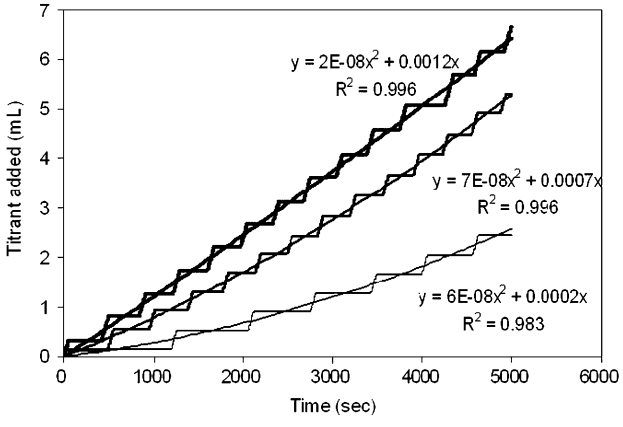

Fig. 1. Illustrative data obtained from pH-stat system in the absence and presence of different concentrations of phosphate. Stepwise data are recorded by the pH-stat system; smooth curves are quadratic regressions of stepwise data (C_T/Ca = 1, I = 0.1, 25 °C).

2.2. Calculation of speciation in the solution phase and on the calcite surface

The soluble chemical speciation and calcite surface speciation under our experimental conditions were determined by Visual MINTEQ version 2.30 (Gustafsson, 2004). Table 2 summarizes the thermodynamic data for the solution-phase reactions considered in these calculations. With respect to reactions at the calcite surface, knowledge of the charge on the calcite surface in the absence of phosphate is crucial for understanding adsorption reactions. Calculation of the calcite surface speciation under our experimental conditions was based on the surface complexation model originally proposed by van Cappellen et al. (1993) and later modified by Pokrovsky et al. (2000). The surface complexation reactions and their intrinsic stability constants, K^{o}_{int}, used in these calculations are also shown in Table 2. Surface densities for both calcium and carbonate sites were assigned to be 5 sites/nm^2 (Davis and Kent, 1990) for the calcite crystal employed. A constant capacitance model, with a double layer capacitance of $I^{1/2}$/0.006 (F/m^2, I is ionic strength) was used for the calculation of surface potential (Pokrovsky et al., 2000). The surface sites were presumed to be distributed homogeneously on the calcite surface.

Table 2
Thermodynamic data for solution-phase and surface complexation reactions used for chemical speciation analysis

Solution-phase reactions	log K	Source
(1) $H^+ + CO_3^{2-} = HCO_3^-$	10.329	[a]
(2) $2H^+ + CO_3^{2-} = H_2CO_{3(aq)}$	16.681	[a]
(3) $Ca^{2+} + H^+ + CO_3^{2-} = CaHCO_3^+$	11.599	[a]
(4) $Ca^{2+} + CO_3^{2-} = CaCO_{3(aq)}^0$	3.2	[a]
(5) $Na^+ + CO_3^{2-} = NaCO_3^-$	1.27	[a]
(6) $Na^+ + H^+ + CO_3^{2-} = NaHCO_{3(aq)}^0$	10.079	[a]
(7) $H^+ + PO_4^{3-} = HPO_4^{2-}$	12.375	[a]
(8) $2H^+ + PO_4^{3-} = H_2PO_4^-$	19.597	[a]
(9) $3H^+ + PO_4^{3-} = H_3PO_4$	21.721	[a]
(10) $Ca^{2+} + PO_4^{3-} = CaPO_{4(aq)}^0$	6.46	[b]
(11) $Ca^{2+} + H^+ + PO_4^{3-} = CaHPO_{4(aq)}^0$	15.035	[a]
(12) $Ca^{2+} + 2H^+ + PO_4^{3-} = CaHPO_4^+$	20.923	[a]
(13) $Na^+ + H^+ + PO_4^{3-} = NaHPO_4^-$	13.445	[a]
(14) $K^+ + H^+ + PO_4^{3-} = KHPO_4^-$	13.255	[a]
(15) $Ca^{2+} + OH^- = CaOH^+$	−12.697	[a]
(16) $Ca^{2+} + Cl^- = CaCl^+$	0.2	[a]
Calcite/water surface complexation reactions[d]	**log K^{o}_{int}**	**Source**
(17) $>CaOH + H^+ = >CaOH_2^{+e}$	11.5	[c]
(18) $>CaOH = >CaO^- + H^+$	−12	[c]
(19) $>CaOH + CO_3^{2-} + 2\,H^+ = >CaHCO_3^0 + H_2O$	23.5	[c]
(20) $>CaOH + CO_3^{2-} + H^+ = >CaCO_3^- + H_2O$	17.1	[c]
(21) $>CO_3H = >CO_3^- + H^+$	−5.1	[c]
(22) $>CO_3H + Ca^{2+} = >CO_3Ca^+ + H^+$	−1.7	[c]

[a] Martell et al. (1997); [b] SC-Database (1998); [c] Pokrovsky et al. (2000); [d] I = 0, 25 °C; [e] >symbolizes mineral surface.

3. Results and discussion

3.1. Kinetics of calcite precipitation in the presence of phosphate

The reduction in the rate of calcite precipitation by phosphate was studied for four different solution compositions with the same degree of supersaturation ($\Omega = 5.3$) at 25 °C. The precipitation rate and the relative reduction in the precipitation rate, expressed as R_i/R_o (R_o is the precipitation rate in the absence of phosphate and R_i is the precipitation rate in the presence of phosphate), as a function of initial total phosphate concentration are shown in Fig. 2. The precipitation rates determined in this study are comparable to those determined by Reddy (1977), given the similar degree of supersaturation employed in both studies. Phosphate showed a stronger inhibitory effect on calcite precipitation at the lower C_T/Ca^{2+} ratios or at the lower pH values. We use initial total phosphate concentration to analyze our data, instead of using final phosphate concentration as suggested by some researchers (Mucci, 1986; Burton and Walter, 1990), because the final phosphate concentration may not truly reflect the impact of phosphate on the initial precipitation rate.

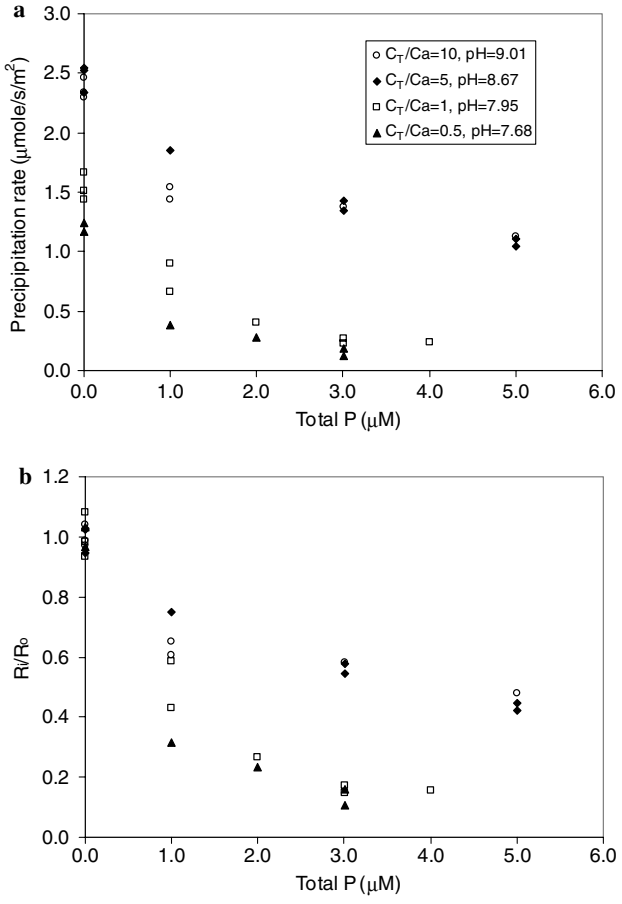

Fig. 2. (a) Inhibition of calcite precipitation as a function of initial total phosphate concentration at 25 °C. (b) Relative rate of calcite precipitation (R_i/R_0) as a function of initial total phosphate concentration.

X-ray diffraction analysis indicated that calcite was the only calcium carbonate crystalline phase present. Although the solutions were also oversaturated with respect to calcium hydroxyapatite (HAP, $K_{sp} = 10^{-3.421}$ at 25 °C) with a degree of oversaturation of $10^{6.26}$–$10^{6.65}$, the precipitation of HAP is kinetically unlikely as suggested by Plant and House (2002) who showed that the homogeneous nucleation of HAP occurred only at degrees of oversaturation greater than $10^{9.4}$ and that the presence of calcite seed was unable to promote heterogeneous nucleation of HAP even at a supersaturation ratio of 10^{14}.

3.2. Mechanism of inhibition of calcite precipitation by phosphate

To simulate the interaction between phosphate and the calcite surface and the impact of phosphate on calcite precipitation kinetics in our experiments, we assumed that the adsorption of phosphate on the calcite surface follows a simple Langmuir adsorption model, because a plateau or the trend to approach a plateau in the calcite precipitation rate was observed as the total initial dissolved phosphate concentration increased for all solution compositions studied (Fig. 2). The interaction between phosphate and calcite can be described by the following equation:

$$> S^-\text{-}nH_2O + P = \ > S^-\text{-}P + nH_2O$$

$$K_{cond} = \frac{[> S^-\text{-}P]}{[> S^-\text{-}nH_2O][P]}, \quad (2)$$

where $>S^-\text{-}nH_2O$ represents the hydrated free active crystal-growth sites on the calcite surface, $>S^-$-P represents the sites at which phosphate is adsorbed, P represents total dissolved phosphate, brackets represent the concentration of each species (units for surface species and soluble species are μmol/m^2 and μM, respectively), and K_{cond} is a "conditional" equilibrium constant. Phosphate is assumed to replace adsorbed water molecules and perhaps undergoes dehydration at the calcite surface (House et al., 1986). The reason we assign a negative charge to the hydrated free active crystal-growth sites is that, from our earlier work (Lin and Singer, 2005), the active crystal-growth sites on the calcite surface were identified to be $>CaCO_3^-$ and $>CO_3^-$, and they are expected to exhibit similar reactivity in the presence of foreign ions. The concentration of the hydrated free active crystal-growth sites in the presence of phosphate can be expressed as:

$$[>S^-\text{-}nH_2O] = \frac{[>S^-\text{-}nH_2O]_T}{1 + K_{cond}[P]}, \quad (3)$$

where $[>S^-\text{-}nH_2O]_T$ represents the total hydrated active crystal-growth sites before phosphate adsorption (μmol/m^2). Assuming that the calcite precipitation rate is proportional to the concentration of available active sites on the calcite surface, the effect of varying total phosphate

concentration on the precipitation rate can then be expressed by the following equation:

$$\frac{R_0 - R_i}{R_i} = K_{cond}[P], \quad (4)$$

where R_0 is the calcite crystal-growth rate in the absence of phosphate and R_i is the inhibited calcite crystal-growth rate in the presence of phosphate. A similar expression has been used successfully to model the impacts of various ionic species on calcite precipitation, such as phosphorus-containing anions (Reddy, 1977); metal ions (Reddy and Wang, 1980; Meyer, 1984; Dromgoole and Walter, 1990) and natural organic matter (Lin et al., 2005).

Fig. 3 shows a plot of $(R_0 - R_i)/R_i$ vs. [P] for all solution compositions investigated in this study, with all regression lines forced through zero. We observed linear relationships between $(R_0 - R_i)/R_i$ and [P] ($R^2 = 0.79 - 0.99$) for each set of conditions suggesting that simple Langmuir adsorption can be used to describe the effect of phosphate on calcite precipitation kinetics. The slopes of these linear relationships are the conditional equilibrium constants, K_{cond}. In general, the values of K_{cond} increase with decreasing C_T/Ca^{2+} ratio or pH value.

Blockage of active crystal-growth sites by adsorbed phosphate has been widely accepted to be responsible for the reduced rate of calcite precipitation (Reddy, 1977; House and Donaldson, 1986; Mucci, 1986; Giannimaras and Koutsoukos, 1987; Burton and Walter, 1990). However, the literature gives conflicting evidence as to which isotherm models can best describe phosphate adsorption onto calcite. Reddy (1977) and Giannimaras and Koutsoukos (1987) reported that a simple Langmuirian model could be used to describe the reduction of the calcite precipitation rate in the presence of phosphate in fresh water at pH values of 8.8 and 8.5, respectively. House and Donaldson (1986) showed that a two-component Langmuirian model, involving the competition between PO_4^{3-} (or $CaPO_4^-$) and HPO_4^{2-} (or $CaHPO_4^0$) for the same sites on the calcite surface, best described the pH-dependent adsorption of phosphate in fresh water from pH 7 to 9.5. De Kanel and Morse (1978) and Mucci (1986) studied the adsorption of phosphate on calcite and the inhibition of calcite precipitation by phosphate in simulated seawater solutions. They found that only the Elovichian chemisorption theory, which assumes an exponential decrease in the available adsorption sites over time, could satisfactorily describe their data because of the absence of an observable plateau in their plots of adsorbed phosphate concentration versus dissolved phosphate concentration. The discrepancy among the modeling results in these studies (including the present study) is most likely due to the different adsorption behavior of phosphate on the calcite surface in fresh water and in seawater-like solutions.

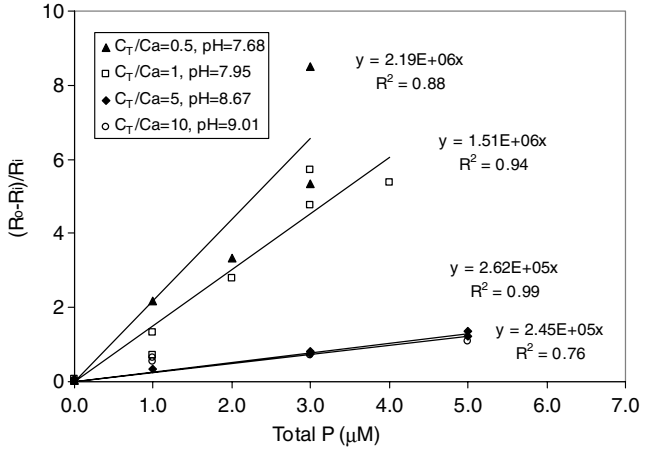

Fig. 3. Inhibition of calcite precipitation by phosphate in accordance with Eq. (4). Slope is the value of the conditional equilibrium constant K_{cond}.

3.3. Key reaction for the inhibition of calcite precipitation by phosphate

It should be noted that for any chemical reaction, the equilibrium constant should indeed be a "constant" for any given temperature and pressure (25 °C and 1 atm, respectively, in our experiments). The "conditional" nature of the K_{cond} values shown in Fig. 3 must result from the fact that only certain phosphate species are involved in the adsorption reaction, rather than total phosphate. As shown in Table 2, there are nine possible phosphate-containing species in our experimental system; the total phosphate concentration is a summation of the concentration of each of these nine species:

$$[P] = [H_3PO_4] + [H_2PO_4^-] + [HPO_4^{2-}] + [PO_4^{3-}] + [CaH_2PO_4^+] + [CaHPO_4^0] + [CaPO_4^-] + [NaHPO_4^-] + [KHPO_4^-] \quad (5)$$

Because the interaction between phosphate and calcite is somewhat electrostatic in nature (Giannimaras and Koutsoukos, 1987), it is likely that not all of the phosphate species shown in Eq. (5) contribute to phosphate adsorption. If the responsible species are identified, the conditional equilibrium constant obtained by Eq. (4) and Fig. 3 may converge to a single "non-conditional" equilibrium constant. To determine the responsible species, we plotted $(R_0 - R_i)/R_i$ vs. the activity of each species as shown in Fig. 4 (H_3PO_4 is not shown due to it low activity, $<10^{-12}$). An examination of all the plots in Fig. 4 shows that only those for ($CaHPO_{4(aq)}^0$) and ($H_2PO_4^-$) (parenthesis denotes activity) converge toward one K value for all C_T/Ca^{2+} conditions tested, suggesting that both $CaHPO_{4(aq)}^0$ and $H_2PO_4^-$ could be the responsible species that adsorb on the calcite surface and inhibit calcite precipitation. However, the surface sites responsible for calcite precipitation are shown to be $>CaCO_3^-$ and $>CO_3^-$ (Lin and Singer, 2005), and the surface charge of calcite is negative under most of our experimental conditions as determined by calcite surface complexation modeling (see Fig. 3(b) in Lin et al. (2005)). Hence, it is expected that the negatively charged $H_2PO_4^-$ species should have less

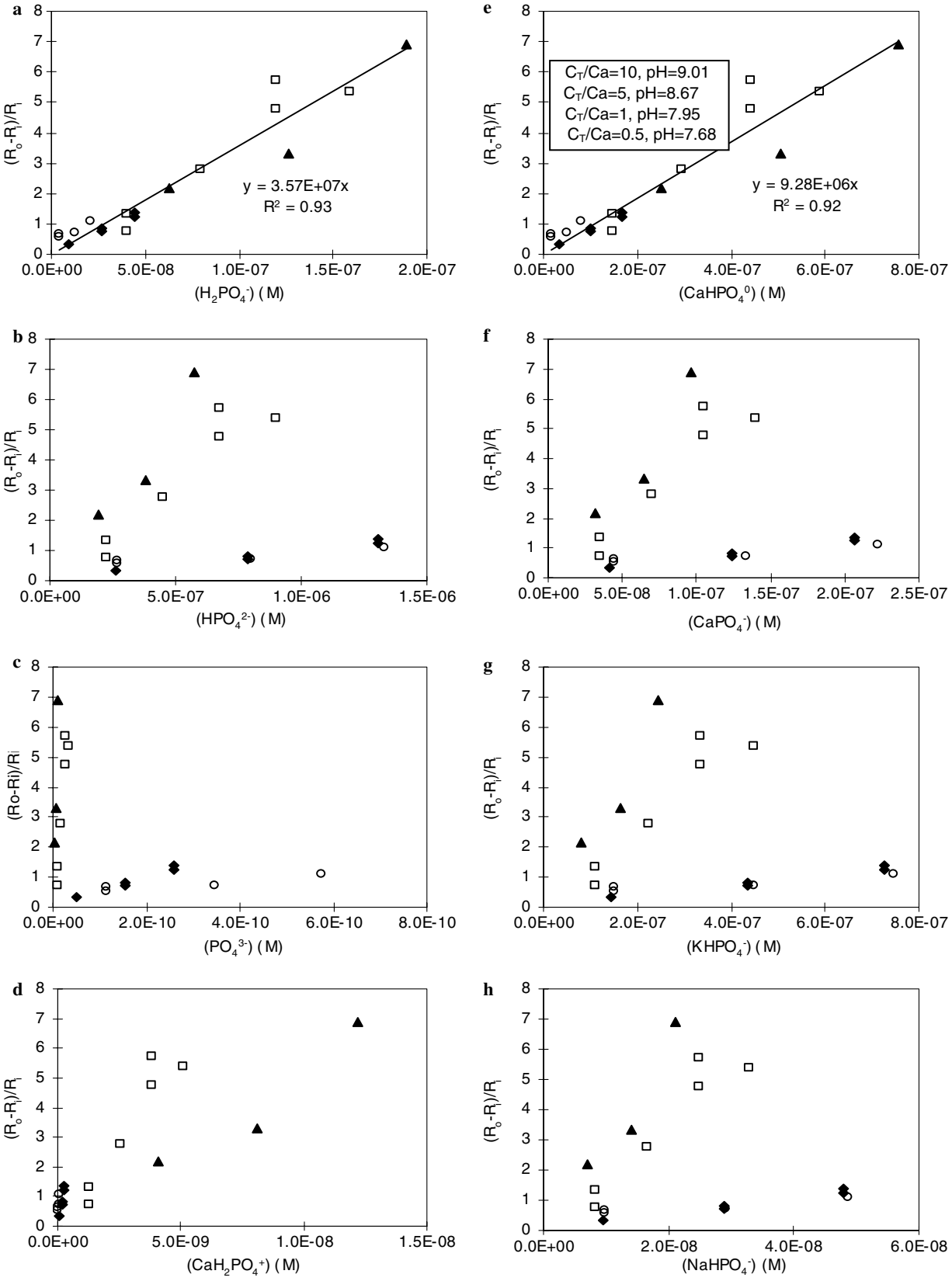

Fig. 4. Inhibition of calcite precipitation in accordance with Eq. (4) as a function of the calculated activity of each phosphate species in the system. The convergence of data points using ($CaHPO_{4(aq)}^{0}$) (e) and ($H_2PO_4^-$) (a) suggests that both $CaHPO_{4(aq)}^{0}$ and $H_2PO_4^-$ are possible species responsible for inhibiting calcite precipitation.

affinity toward the negatively charged calcite surface and should not be extensively adsorbed. In fact, the convergence of the plot using $H_2PO_4^-$ might simply result from the linear correlation between $(H_2PO_4^-)$ and $(CaHPO_{4(aq)}^0)$. According to reactions (8) and (11) in Table 2, $(H_2PO_4^-)$ is correlated to $(CaHPO_{4(aq)}^0)$ through the following relationship:

$$\left(H_2PO_4^-\right) = \frac{K_8}{K_{11}} \frac{(H^+)}{(Ca^{2+})} \left(CaHPO_{4(aq)}^0\right), \quad (6)$$

where K_i represents the equilibrium constant for reaction (i) in Table 2.

From Eq. (1) and reactions (1) and (2) in Table 2, Eq. (6) can be rewritten as:

$$\left(H_2PO_4^-\right) = \frac{K_8}{K_{11}} \frac{\gamma_{CO_3^{2-}} \cdot C_T \cdot \alpha_2 \cdot (H^+)}{\Omega \cdot K_{sp}} \left(CaHPO_{4(aq)}^0\right), \quad (7)$$

where $\gamma_{CO_3^{2-}}$ is the activity coefficient for CO_3^{2-} and α_2 is a distribution function for carbonic acid (Stumm and Morgan, 1996), which can be expressed as follows:

$$\alpha_2 = \frac{1}{K_2(H^+)^2 + K_1(H^+) + 1}. \quad (8)$$

Since $\gamma_{CO_3^{2-}}$, C_T, Ω, and K_{sp} are all constants under our experimental conditions, and the value of $\alpha_2 \cdot (H^+)$ is also close to being constant for pH values varying from 7.68 to 9.01 (minimum of 4.46×10^{-11} at pH 9.01; maximum of 4.59×10^{-11} at pH 8.30), a linear relationship between $H_2PO_4^-$ and $(CaHPO_{4(aq)}^0)$ is expected, i.e., $(CaHPO_{4(aq)}^0) \approx 4(H_2PO_4^-)$.

Based on the above analysis, we believe that $CaHPO_{4(aq)}^0$ is the primary species that adsorbs on the calcite surface and inhibits calcite precipitation, although $H_2PO_4^-$ and other negatively charged species might still contribute to a small fraction of phosphate adsorption through an anion exchange mechanism (Ishikawa and Ichikuni, 1981; House and Donaldson, 1986). The reaction responsible for the adsorption of phosphate and the subsequent inhibition of calcite precipitation can therefore be expressed as follows:

$$>S^-\text{-}nH_2O + CaHPO_{4(aq)}^0 = >S^-\text{-}CaHPO_4^0 + nH_2O$$
$$K_{CaHPO_4^0} = 9.28(\pm 0.93) \times 10^6, \quad (9)$$

where $K_{CaHPO_4^0}$ is a "non-conditional" equilibrium constant for the site-specific reaction and its value, shown in Eq. (9) with 95% confidence limits, can be obtained from the slope of Fig. 4(e). Accordingly, the effect of varying total phosphate concentrations on the calcite precipitation rate can be expressed by the following equation:

$$\frac{R_0 - R_i}{R_i} = K_{CaHPO_{4(aq)}^0} \left(CaHPO_{4(aq)}^0\right). \quad (10)$$

The importance of Eq. (9) in the inhibition of calcite precipitation is further demonstrated in Fig. 5, where the calcite precipitation rate (Fig. 2(a)) is plotted as a function of the residual active crystal-growth site concentration $([>CaCO_3^-] + [>CO_3^-])_{active}$ after phosphate adsorption. The residual active crystal-growth site concentration is calculated from the site concentration $[>CaCO_3^-] + [>CO_3^-]$ before phosphate adsorption minus the sites occupied by $(CaHPO_{4(aq)}^0)$ as determined using Eq. (9). The linear relationship ($y = 1.3x$, $R^2 = 0.88$) between the calcite precipitation rate and $([>CaCO_3^-] + [>CO_3^-])_{active}$ strongly suggests that $CaHPO_{4(aq)}^0$ is the only important species that blocks active crystal-growth sites, and that those active sites responsible for calcite precipitation are $>CaCO_3^-$ and $>CO_3^-$ as suggested by Lin and Singer (2005).

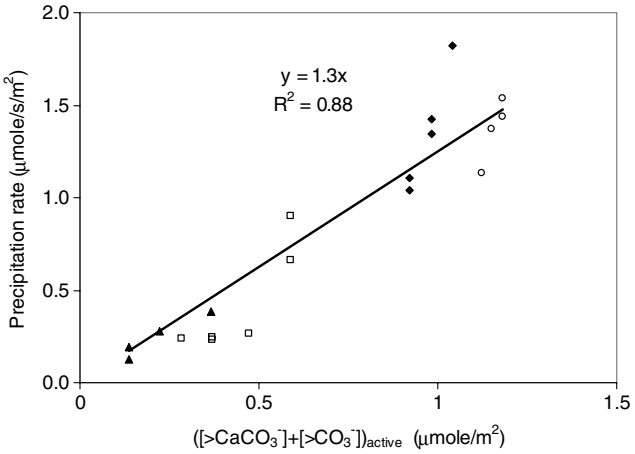

Fig. 5. Calcite precipitation rate in the presence of phosphate (R_i) as a function of the concentration of active crystal-growth sites $([>CaCO_3^-] + [>CO_3^-])_{active}$.

3.4. Thermodynamics of phosphate adsorption on the calcite surface

In order to determine the thermodynamic parameters of the reaction described in Eq. (9), we performed additional pH-stat experiments from 15 to 45 °C using solutions with the same degree of supersaturation ($\Omega = 5.3$, Table 1). The calcite precipitation rate and the relative reduction in precipitation rates as a function of initial total phosphate concentration for different temperatures are shown in Fig. 6. The plots of $(R_0 - R_i)/R_i$ vs. $(CaHPO_{4(aq)}^0)$ used for determining the value of $K_{CaHPO_4^0}$ for each temperature are shown in Fig. 7.

The standard free energy (ΔG^0) for the reaction can be estimated from the following equation:

$$\Delta G^0 = -RT \ln K_{CaHPO_{4(aq)}^0}, \quad (11)$$

where R is the ideal gas constant and T is the absolute temperature.

The standard enthalpy change (ΔH^0) for the reaction can be estimated by the values of $K_{CaHPO_4^0}$ determined at different temperatures using the integrated form of the van't Hoff equation:

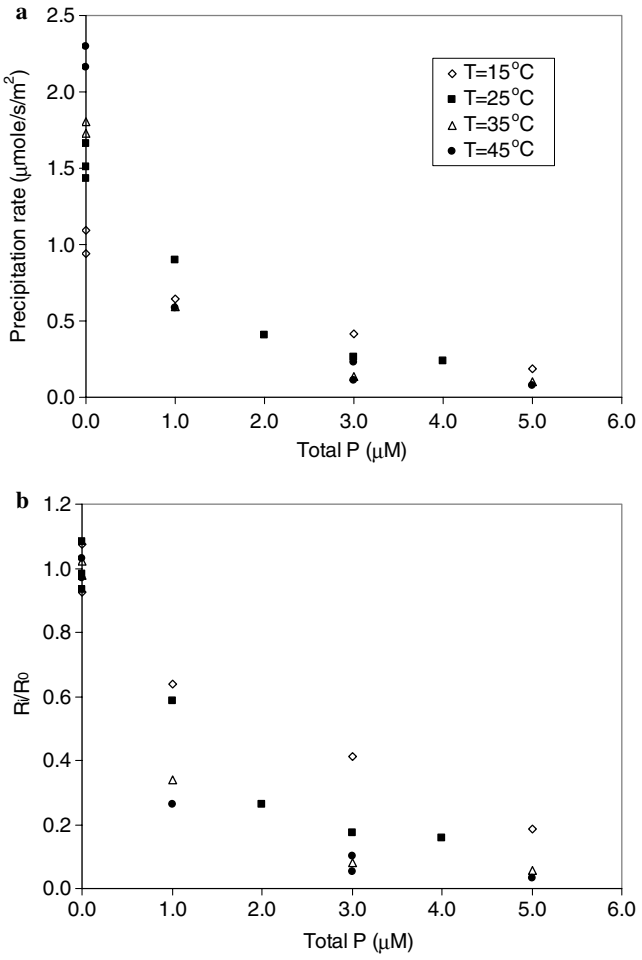

Fig. 6. (a) Inhibition of calcite precipitation as a function of initial total phosphate concentration at different temperatures (b) Relative rate of calcite precipitation (R_i/R_0) as a function of initial total phosphate concentration at different temperatures.

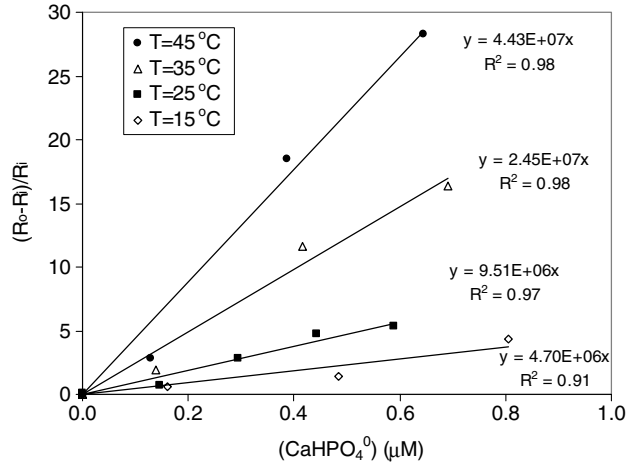

Fig. 7. Inhibition of calcite precipitation by phosphate at different temperatures in accordance with Eq. (10).

$$\ln K_{\mathrm{CaHPO_{4(aq)}}^{0}} = -\frac{\Delta H^0}{RT} + C, \tag{12}$$

where C is the constant of integration.

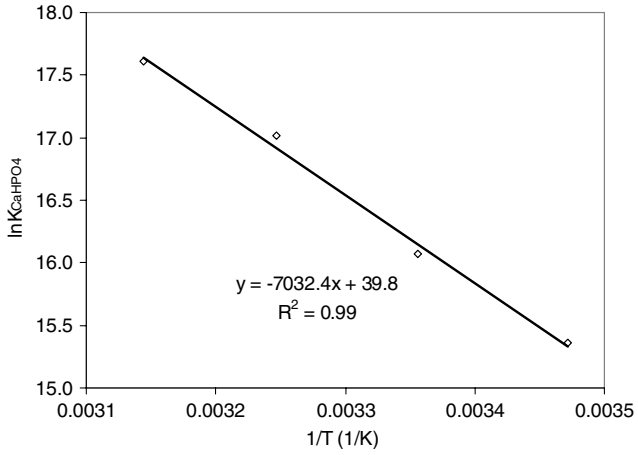

Fig. 8. van't Hoff plot of non-conditional stability constant $\mathrm{CaHPO_{4(aq)}}^{0}$ at different temperatures. Slope is equal to $-\Delta H^0/R$.

ΔH^0 is assumed to be independent of temperature because of the low concentrations of phosphate (1–5 μM) and the narrow temperature range (15–45 °C) employed in our experiments. The plot of $\ln K_{\mathrm{CaHPO_{4(aq)}}^{0}}$ vs. T^{-1} in accordance with Eq. (12) is shown in Fig. 8. A good linear relationship between $\ln K_{\mathrm{CaHPO_{4(aq)}}^{0}}$ and T^{-1} was observed ($R^2 = 0.99$). The slope of the plot of $\ln K_{\mathrm{CaHPO_{4(aq)}}^{0}}$ vs. T^{-1} is equal to $\Delta H^0/R$ according to Eq. (12).

The standard free energy change contributed by the standard entropy change ($T\Delta S^0$) can be calculated from the following equation:

$$T\Delta S^0 = \Delta H^0 - \Delta G^0. \tag{13}$$

Thermodynamic data for the adsorption reaction (Eq. (9)) calculated from Eqs. (11) to (13) are summarized in Table 3. House and Donaldson (1986) documented that the enthalpy change for the adsorption of HPO_4^{2-} onto calcite was 43.5 kJ/mol. The smaller value they obtained most likely results from an incomplete analysis of solution speciation, e.g., omission of important sorptive species such as $\mathrm{CaHPO_{4(aq)}}^{0}$. The high positive values of ΔH^0 (58.5 kJ/mol) and $T\Delta S^0$ (98.3 kJ/mol) from our analysis suggest that the adsorption of $\mathrm{CaHPO_{4(aq)}}^{0}$ onto active calcite crystal-growth sites is endothermic, chemisorptive in nature, and driven solely by entropy change, most likely resulting from the release of water molecules from the calcite surface to compensate for the adsorption of $\mathrm{CaHPO_{4(aq)}}^{0}$. The chemisorptive nature also explain why $\mathrm{CaHPO_{4(aq)}}^{0}$, a neutral species, has a strong affinity for the negatively charged calcite surface.

Table 3
Summary of thermodynamic data for the adsorption of $\mathrm{CaHPO_{4(aq)}}^{0}$ onto calcite (25 °C, 1 atm) (all units are kJ/mol)

ΔG^0	ΔH^0	$T\Delta S^0$
−39.8	58.5	98.3

3.5. Phosphate inhibition mechanisms based upon empirical kinetic models, in situ surface imaging techniques, and surface complexation models

Two other major routes for interpreting the effects of impurities on calcite precipitation kinetics arise from studies based upon: (1) empirical kinetic models (Mucci, 1986; House, 1987; Burton and Walter, 1990) and (2) in situ surface imaging techniques, such as atomic force microscopy (AFM) or scanning force microscopy (SFM) (Dove and Hochella, 1993; Davis et al., 2000; Orme et al., 2001; Astilleros et al., 2002)

The use of an empirical kinetic model to interpret precipitation inhibition kinetics relies on the success of the empirical rate expression shown in Eq. (14) to describe experimental observations, with Ω as the sole variable (Morse, 1983):

$$R = k(\Omega - 1)^n, \tag{14}$$

where k and n are the empirical rate constant and reaction order, respectively.

Many researchers have attempted to correlate the empirical reaction order to surface processes involved in calcite precipitation (Nancollas and Reddy, 1971; Reddy and Gaillard, 1981; Nielsen, 1983; Blum and Lasaga, 1987; Shiraki and Brantley, 1995). However, we have shown that Eq. (14) failed to model calcite precipitation kinetics for solutions with the same degree of supersaturation but different C_T/Ca^{2+} ratios, such as those used in this study (Lin and Singer, 2005). More importantly, an atomic force microscopy study demonstrated that Eq. (14) cannot be simply used to correlate any growth processes that occur at mineral surfaces (Teng et al., 2000). Thus, using an empirical kinetic model to further explain the effects of inhibitors on calcite precipitation will provide limited mechanistic information.

The use of AFM or SFM significantly improves the understanding of surface processes during calcite precipitation. Usually AFM and SFM provide images that capture the advances of steps and changes in surface morphology as a function of time, which allow for the calculation of step velocity and in situ observation of surface processes during precipitation. Teng et al. (2000) showed that for solutions in the absence of an inhibitor, with Ω less than about 2, calcite crystal growth proceeds by step flow at surface defects, while for solutions with Ω greater than 2, two-dimensional surface nucleation become increasingly important. Considering the supersaturation state of our working solutions ($\Omega = 5.3$), it leads us to believe that the adsorption of $CaHPO_{4(aq)}^{\ 0}$ on the calcite surface alters the formation and subsequent growth of surface nuclei, and results in the reduced precipitation kinetics we observed. In fact, a study by Dove and Hochella (1993) using SFM showed that the influence of phosphate on calcite precipitation depends on calcite surface history in solution with supersaturation ratios greater than 2. If phosphate is introduced during the surface nucleation stage, surface nuclei show amorphous shapes; if phosphate is introduced during layer growth, relatively straight steps become jagged ones.

It should be noted that the details of surface speciation cannot be revealed by AFM or SFM, and the use of surface complexation modeling requires a simplifying assumption that active growth sites are distributed uniformly on the calcite surface. This assumption obviously needs modification, for example, by assigning a higher activity to those sites located at surface defects due to their higher surface energies (Mullin, 2001). A more precise description of the effects of phosphate and other impurities on calcite precipitation kinetics in terms of both surface speciation and surface processes may be developed by combining direct surface observations and surface complexation modeling.

4. Conclusions

Through a detailed analysis of solution speciation and surface speciation in solutions containing calcium, carbonate, phosphate and suspended calcite seed, $CaHPO_{4(aq)}^{\ 0}$ was found to be the responsible species that adsorbs on the calcite surface and inhibits calcite precipitation. The reduction in the calcite precipitation rate by phosphate can be interpreted in terms of a Langmuir adsorption model using active crystal-growth sites and $CaHPO_{4(aq)}^{\ 0}$ as the adsorbing species. The standard enthalpy change and standard entropy change for the adsorption reaction suggest that the reaction is a chemisorption process, and that the adsorption is an endothermic reaction driven by the entropy change, most likely resulting from the dehydration process on the calcite surface.

Acknowledgments

The authors thank Procter and Gamble for supporting this research, and three anonymous reviewers for their valuable comments on this article.

Associate editor: John Morse

References

Astilleros, J.M., Pina, C.M., Fernandez-Diaz, L., Putnis, A., 2002. Molecular-scale surface processes during the growth of calcite in the presence of manganese. *Geochim. Cosmochim. Acta* **66** (18), 3177–3189.

Berg, U., Neumann, T., Donnert, D., Nuesch, R., Stuben, D., 2004. Sediment capping in eutrophic lakes—efficiency of undisturbed calcite barriers to immobilize phosphorus. *Appl. Geochem.* **19** (11), 1759–1771.

Blum, A.E., Lasaga, A.C., 1987. Monte Carlo simulations of surface reaction rate laws. In: Stumm, W. (Ed.), *Aquatic Surface Chemistry*. Wiley.

Brunauer, S., Emmet, P.H., Teller, E., 1938. Adsorption of gases in multimolecular layers. *J. Am. Chem. Soc.* **60**, 309–319.

Burton, E.A., Walter, L.M., 1990. The role of pH in phosphate inhibition of calcite and aragonite precipitation rates in seawater. *Geochim. Cosmochim. Acta* **54** (3), 797–808.

Davis, J.A., Kent, D.B., 1990. Surface complexation modeling in aqueous geochemistry. In: Hochella, M.F., White, A.F. (Eds.), *Mineral–Water Interface Geochemistry*. Mineralogical Society of America, Washington, DC, pp. 177–260.

Davis, K.J., Dove, P.M., De Yoreo, J.J., 2000. The role of Mg^{2+} as an impurity in calcite growth. *Science* **290** (5494), 1134–1137.

De Kanel, J., Morse, J.W., 1978. The chemistry of orthophosphate uptake from seawater onto calcite and aragonite. *Geochim. Cosmochim. Acta* **42**, 1335–1340.

Dittrich, M., Koschel, R., 2002. Interactions between calcite precipitation (natural and artificial) and phosphorus cycle in the hardwater lake. *Hydrobiologia* **469** (1–3), 49–57.

Dittrich, M., Dittrich, T., Sieber, I., Koschel, R., 1997. A balance analysis of phosphorus elimination by artificial calcite precipitation in a stratified hardwater lake. *Water Res.* **31** (2), 237–248.

Dove, P.M., Hochella, M.F., 1993. Calcite precipitation mechanisms and inhibition by orthophosphate: in situ observations by scanning force microscopy. *Geochim. Cosmochim. Acta* **57** (3), 705–714.

Dromgoole, E.L., Walter, L.M., 1990. Inhibition of calcite growth rates by Mn^{2+} in $CaCl_2$ solutions at 10, 25, and 50 °C. *Geochim. Cosmochim. Acta* **54** (11), 2991–3000.

Evans, D.J., Johnes, P., 2004. Physico-chemical controls on phosphorus cycling in two lowland streams. Part 1—the water column. *Sci. Total Environ.* **329** (1–3), 145–163.

Evans, D.J., Johnes, P.J., Lawrence, D.S., 2004. Physico-chemical controls on phosphorus cycling in two lowland streams. Part 2—the sediment phase. *Sci. Total Environ.* **329** (1–3), 165–182.

Giannimaras, E.K., Koutsoukos, P.G., 1987. The crystallization of calcite in the presence of orthophosphate. *J. Colloid Interface Sci.* **116** (2), 423–430.

Gustafsson, J.P., 2004. Visual MINTEQ ver. 2.30. (http://www.lwr.kth.se/english/OurSoftWare/Vminteq/). Department of Land and Water Resources Engineering, The Royal Institute of Technology in Stockholm.

House, W.A., 1987. Inhibition of calcite crystal growth by inorganic phosphate. *J. Colloid Interface Sci.* **119** (2), 505–511.

House, W.A., 2003. Geochemical cycling of phosphorus in rivers. *Appl. Geochem.* **18** (5), 739–748.

House, W.A., Denison, F.H., 2002. Exchange of inorganic phosphate between river waters and bed sediments. *Environ. Sci. Technol.* **36** (20), 4295–4301.

House, W.A., Donaldson, L., 1986. Adsorption and coprecipitation of phosphate on calcite. *J. Colloid Interface Sci.* **112** (2), 309–324.

House, W.A., Casey, H., Donaldson, L., Smith, S., 1986. Factors affecting the coprecipitation of inorganic phosphate with calcite in hardwaters. 1. Laboratory studies. *Water Res.* **20** (7), 917–922.

Ishikawa, M., Ichikuni, M., 1981. Coprecipitation of phosphate with calcite. *Geochem. J.* **15** (5), 283–288.

Jensen, H.S., Mortensen, P.B., Andersen, F.O., Rasmussen, E., Jensen, A., 1995. Phosphorus cycling in a coastal marine sediment, Aarhus Bay, Denmark. *Limnol. Oceanogr.* **40** (5), 908–917.

Kotak, B.G., Lam, A.K.Y., Prepas, E.E., Kenefick, S.L., Hrudey, S.E., 1995. Variability of the hepatotoxin microcystin-LR in hypereutrophic drinking water lakes. *J. Phycol.* **31** (2), 248–263.

Lin, Y.P., Singer, P.C., 2005. Effects of seed material and solution composition on calcite precipitation. *Geochim. Cosmochim. Acta* **69** (18), 4495–4504.

Lin, Y.P., Singer, P.C., Aiken, G.R., 2005. Inhibition of calcite precipitation by natural organic materials: kinetics, mechanism and thermodynamics. *Environ. Sci. Technol.* **39** (17), 6420–6428.

Martell, A.E., Smith, R.M., Motekaitis, R.J., 1997. Critically selected stability constants of metal complexes, Version 4; U.S. Department of Commerce, National Institute of Standards and Technology, Gaithersbug, MD.

Meyer, H.J., 1984. The influence of impurities on the growth rate of calcite. *J. Cryst. Growth* **66** (3), 639–646.

Millero, F., Huang, F., Zhu, X.R., Liu, X.W., Zhang, J.Z., 2001. Adsorption and desorption of phosphate on calcite and aragonite in seawater. *Aquat. Geochem.* **7** (1), 33–56.

Morse, J.W., 1983. The kinetics of calcium carbonate dissolution and precipitation. In: Reeder, R.J. (Ed.), *Carbonates: Mineralogy and Chemistry Reviews in Mineralogy*, vol. 11. Mineralogical Society of America, pp. 227–264.

Mucci, A., 1986. Growth kinetics and composition of magnesian calcite overgrowths precipitated from seawater— quantitative influence of ortho-phosphate ions. *Geochim. Cosmochim. Acta* **50** (10), 2255–2265.

Mullin, J.W., 2001. *Crystallization*. Butterworth-Heinemann.

Nancollas, G.H., Reddy, M.M., 1971. The crystallization of calcium carbonate II. Calcite growth mechanism. *J. Colloid Interface Sci.* **37** (4), 824–830.

Nielsen, A.E., 1983. Precipitates: formation, coprecipitation, and aging. In: Kolthoff, I.M., Elving, P.J. (Eds.), *Treatise on Analytical Chemistry*. Wiley.

Orme, C.A., Noy, A., Wierzbicki, A., McBride, M.T., Grantham, M., Teng, H.H., Dove, P.M., DeYoreo, J.J., 2001. Formation of chiral morphologies through selective binding of amino acids to calcite surface steps. *Nature* **411** (6839), 775–779.

Plant, L.J., House, W.A., 2002. Precipitation of calcite in the presence of inorganic phosphate. *Colloid Surf. A* **203** (1–3), 143–153.

Pokrovsky, O.S., Mielczarski, J.A., Barres, O., Schott, J., 2000. Surface speciation models of calcite and dolomite/aqueous solution interfaces and their spectroscopic evaluation. *Langmuir* **16** (6), 2677–2688.

Prepas, E.E., Pinel-Alloul, B., Chambers, P.A., Murphy, T.P., Reedyk, S., Sandland, G., Serediak, M., 2001. Lime treatment and its effects on the chemistry and biota of hardwater eutrophic lakes. *Freshwater Biol.* **46** (8), 1049–1060.

Reddy, M.M., 1977. Crystallization of calcium carbonate in the presence of trace concentrations of phosphorous-containing anions: I. Inhibition by phosphate and glycerophosphate ions at pH 8.8 and 25 °C. *J. Cryst. Growth* **41**, 287–295.

Reddy, M.M., Gaillard, W.D., 1981. Kinetics of calcium carbonate (calcite)-seeded crystallization : influence of solid/solution ratio on the reaction rate constant. *J. Colloid Interface Sci.* **80** (1), 171–178.

Reddy, M.M., Wang, K.K., 1980. Crystallization of calcium carbonate in the presence of metal ions. 1. Inhibition by magnesium ion at pH 8.8 and 25 °C. *J. Cryst. Growth* **50** (2), 470–480.

SC-Database. 1998. Stability Constants Database; The International Union of Pure and Applied Chemistry (IUPAC) and Academic Press.

Schindler, D.W., 1974. Eutrophication and recovery in experimental lakes: implications for lake management. *Science* **184** (4139), 897–899.

Shiraki, R., Brantley, S.L., 1995. Kinetics of near equilibrium calcite precipitation at 100 °C: an evaluation of elementary reaction-based and affinity-based rate laws. *Geochim. Cosmochim. Acta* **59** (8), 1457–1471.

Stumm, W., Morgan, J.J., 1996. *Aquatic Chemistry*. Wiley-Interscience, New York.

Teng, H.H., Dove, P.M., De Yoreo, J.J., 2000. Kinetics of calcite growth: Surface processes and relationships to macroscopic rate laws. *Geochim. Cosmochim. Acta* **64** (13), 2255–2266.

van Cappellen, P., Charlet, L., Stumm, W., Wersin, P., 1993. A surface complexation model of the carbonate mineral-aqueous solution interface. *Geochim. Cosmochim. Acta* **57** (15), 3505–3518.

van der Weijden, R.D., Meima, J., Comans, R.N.J., 1997. Sorption and sorption reversibility of cadmium on calcite in the presence of phosphate and sulfate. *Mar. Chem.* **57** (1–2), 119–132.

Walpersdorf, E., Neumann, T., Stuben, D., 2004. Efficiency of natural calcite precipitation compared to lake marl application used for water quality improvement in an eutrophic lake. *Appl. Geochem.* **19** (11), 1687–1698.